Available online at www.sciencedirect.com
SCIENCE DIRECT®
Journal of Nuclear Materials 329–333 (2004) 1233–1237
journal of nuclear materials
www.elsevier.com/locate/jnucmat

Hardening due to copper precipitates in α-iron studied by atomic-scale modelling

D.J. Bacon [a,*], Yu.N. Osetsky [b]

[a] Materials Science and Engineering, Department of Engineering, The University of Liverpool, Brownlow Hill, Liverpool L69 3GH, UK
[b] Oak Ridge National Laboratory, P.O. Box 2008, Oak Ridge, TN 37831-6158, USA

Abstract

We present results of a large-scale atomic-level study of dislocation–precipitate interaction. We have considered a $\frac{1}{2}\langle 1\,1\,1\rangle$ edge dislocation gliding in α-iron containing coherent copper precipitates of size from 0.7 to 6 nm over a temperature range from 0 to 450 K. The results demonstrate that some features are qualitatively consistent with earlier theoretical conclusions, e.g. the critical resolved shear stress (CRSS) is proportional to L^{-1} and $\ln(D)$, where L and D are precipitate spacing and diameter. Other features, which are intrinsic to the atomic-level nature of the dislocation–precipitate interaction, include strong dependence of the CRSS on temperature, dislocation climb and precipitate phase transformation.

1. Introduction

Radiation-induced defects formed under working conditions of metals in the core structures of nuclear power plant are responsible for a significant change in mechanical properties. Examples of extended crystal defects include dislocation loops, voids and secondary phase precipitates: among the latter, precipitates of copper in ferritic alloys are particularly important [1–6]. Such precipitates cause hardening, loss of ductility and increase of ductile-to-brittle transition temperature. Interaction between moving dislocations and precipitates is the cause of these effects and, therefore, understanding of the mechanisms involved is necessary for creation of predictive models of materials properties. This is not a trivial task, the main problem arising from the need to simulate large enough length and time scales in atomic modelling, e.g. lengths of the order of the distance between dislocations and times of the order of dislocation-obstacle interactions under reasonable rates of deformation.

A model developed recently by Osetsky and Bacon [7] resolves the majority of the above problems and is applied here to the study of the interaction between a moving edge dislocation in iron and coherent copper precipitates. The results are compared with previous studies by different techniques and conclusions are made on the importance of treating the problem at atomic scale.

2. Model

The modelling method is described in detail in [7]. In summary, we simulate an infinitely long, straight edge dislocation lying parallel to the y-axis $[1\,1\,\bar{2}]$ with the Burgers vector $\boldsymbol{b}$ along the x-axis $[1\,1\,1]$ gliding in the plane $(1\,\bar{1}\,0)$. Periodic boundary conditions were applied along the x-axis to simulate an array of edge dislocations with period equal to the crystal size, L_b.

The obstacle, consisting of a coherent bcc precipitate of copper atoms, was as near spherical in shape, diameter D, as possible with the equator coinciding with the glide plane $z = 0$ of the dislocation. The periodic

* Corresponding author. Tel.: +44-151 794 4662; fax: +44-151 794 4675.
E-mail address: djbacon@liv.ac.uk (D.J. Bacon).

0022-3115/$ - see front matter © 2004 Elsevier B.V. All rights reserved.
doi:10.1016/j.jnucmat.2004.04.256

boundary conditions along y result in a periodic array of obstacles of spacing L along the dislocation line ($L = 41.5$ nm). Two qualitatively different techniques were used to simulate the dislocation overcoming these obstacles, as follows. In static relaxation ($T = 0$ K), resolved shear strain, ε, was applied incrementally with relaxation to a minimum of the potential energy at each step. In molecular dynamics (MD) simulation ($T > 0$ K), applied shear strain rate, $\dot{\varepsilon}$, was imposed. The details of stress and strain effects on a simulated crystal can be found in [7]. In both the $T = 0$ and $T > 0$ schemes a stress–strain, $\tau(\varepsilon)$, curve is obtained and the maximum value of τ is the critical resolved shear stress (CRSS), τ_c, for the dislocation to move through the array of obstacles.

Crystals of different size $L_b = 30$, 60 and 90 nm, along the x-axis were simulated to test the effect of dislocation–image interaction. The size perpendicular to the dislocation glide plane was equal ~20 nm for all the crystals. The atomic structure of the obstacle and dislocation was analysed at each step of strain increment in static modelling and every 100 time steps in MD (time step $\approx 10^{-15}$ s). Identification and visualisation of the location of the core of the dislocation line is important, and the method used is described in [7]. Finnis–Sinclair type many-body potentials derived by Ackland et al. [8,9] for the Fe–Cu binary system were used for all simulations.

3. Simulation of strengthening at $T = 0$ K

The dependence of the CRSS on precipitate diameter obtained at $T = 0$ is shown in Fig. 1, where it is seen to be close to a linear function of $\ln(D)$. This plot contains data obtained from crystals with different L_b and shows the effect of the simulated crystal size along the direction of b. The CRSS decreases slightly when L_b increases. This dependence may be due to interaction between screw segments formed as the dislocation bows out at the precipitate with their own images. Thus, data for $D = 2$ nm are very similar in all the crystals simulated, indicating a weak effect of image interactions when the dislocation line is not curved strongly and the angle, φ, between its segments that emerge from a precipitate at τ_c is greater than 0°, i.e. the screw component of the line is small. For larger precipitates the dislocation bow out is stronger, the leaving angle φ becomes equal to zero and the influence of image interactions increases. However, the effect of L_b on τ_c is small for the model sizes used here. The critical line shapes for different D are shown in Fig. 2.

Data presented in Fig. 2 present valuable information on the dislocation line shape at τ_c for comparison with models based on the line tension approximation of the dislocation theory. The Russell–Brown (RB) dispersion strengthening model [10] based on earlier isotropic line tension models [11,12] is commonly used for estimating strength due to coherent precipitates. In this model the CRSS is determined by the critical angle, φ, at which a dislocation cuts an obstacle. The comparison of τ_c estimated in this way and that obtained directly from the atomic-scale modelling is presented in Fig. 3. Two qualitative differences are apparent. First, the line tension model overestimates the value of τ_c, demonstrating that the correspondence between the critical angle φ and τ_c in simple theory based on the constant line tension approximation is not correct. This conclusion is not surprising in view of the dislocation line shape presented in Fig. 2, which is very different from the circular arc shape predicted by constant line tension. In fact, as shown earlier [7], the dislocation tends to align with low-index directions, and a similar finding for dislocation

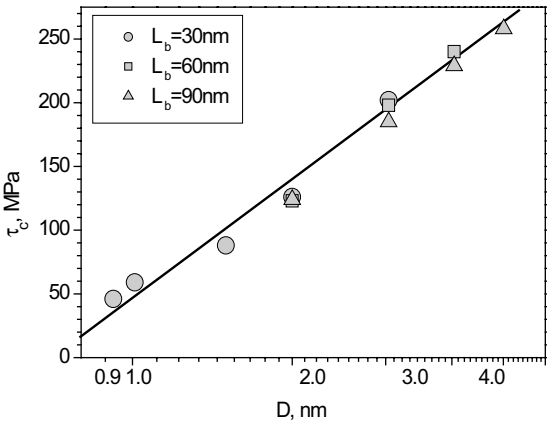

Fig. 1. Dependence of the value of critical resolved shear stress against Cu precipitate diameter. The model dimension L_b is as indicated.

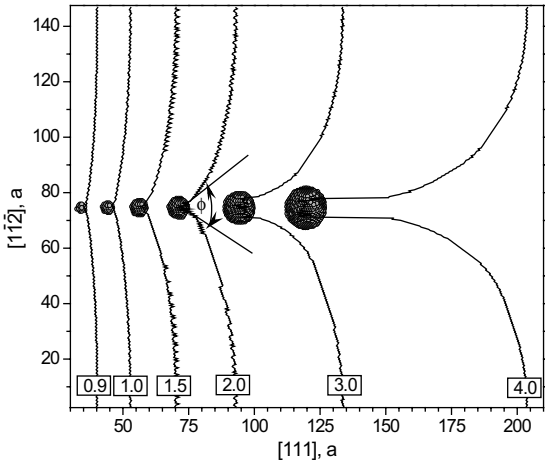

Fig. 2. Dislocation line in the $(1\,\bar{1}\,0)$ slip plane at the critical stress τ_c for different precipitate sizes at 0 K.

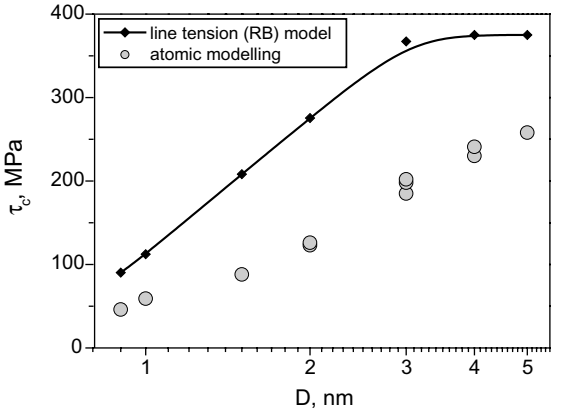

Fig. 3. Comparison of τ_c obtained by atomic modelling (grey circles) and the Russell–Brown model using the critical angles φ from simulation (full diamonds).

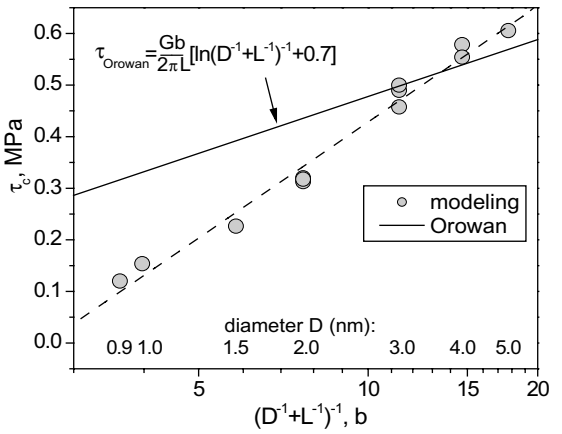

Fig. 4. Critical resolved shear stress τ_c (units Gb/L) versus the harmonic mean of obstacle spacing, L, and diameter, D (units b) for precipitates (grey circles). Solid line shows empirical correlations found by continuum simulation for impenetrable obstacles via the Orowan mechanism [15].

line shape for different L was presented recently for voids [13]. Second, for the line tension model τ_c reaches the limit of the Orowan stress, $\tau_{\text{Orowan}} = 0.8$ Gb/L, when φ approaches zero, whereas in atomic-scale modelling the CRSS increases with D even when φ remains zero. This is a serious weakness of simple line tension models, but can be resolved in more sophisticated dislocation dynamics models when dislocation self-interaction is taken into account.

For example, the τ_c values for precipitate strengthening are compared in Fig. 4, where the critical shear stress, in units of Gb/L, is plotted against the harmonic mean of obstacle spacing and diameter $(D^{-1} + L^{-1})^{-1}$, in units of b. The value of G has been taken as 62.5GPa, which is the effective isotropic shear modulus estimated using anisotropic elasticity for a dislocation of the $\langle 1\,1\,1\rangle$ $\{1\,\bar{1}\,0\}$ glide system in Fe [14]. The harmonic mean has been chosen because such a plot was found to give an excellent correlation for the Orowan stress of a row of impenetrable obstacles in a computer simulation based on elasticity theory in which the self-stress of a flexible dislocation was included explicitly [15]. The rationale for this is that the harmonic mean tends to D when $D \ll L$ and L when $L \ll D$, in recognition that the critical breakaway line configuration of the Orowan process is achieved when the applied stress can draw out a dipole of spacing D (energy $\propto \ln(D)$) when $D \ll L$ and spacing L (energy $\propto \ln(L)$) when $L \ll D$. The solid line in Fig. 4 is the fit obtained in [15] when r_o, the dislocation core cutoff radius used as a unit of length for D and L, is set equal to b. The maximum D simulated here is 5 nm, for which the length of the screw dipole at critical stress is equal to about 140 a. Following the previous discussion, it is possible that this case is affected by the dislocation–image interaction and therefore the actual value of τ_c should be slightly lower than that obtained here. Taking this into account, we observe that the largest precipitates modelled here produce a CRSS close to the Orowan values obtained by continuum self-stress simulation in [15]. Indeed, this is consistent with the mechanism observed provided the critical angle $\varphi = 0$ for $D \geqslant 3$ nm. Simulation of large particles would be necessary to clarify this at significantly larger spacing between the image dislocations i.e. $L_b \gg 100$ nm.

Finally, we note that interaction between a dislocation and coherent bcc precipitates is precipitate-size-dependent, for it provokes a structural transformation in large coherent precipitates, which are metastable with respect to the transformation towards the stable fcc structure. In fact, the Orowan-like line shape, i.e. zero critical angle, but without creation of an Orowan loop around the precipitate, was observed for $D \geqslant 3$ nm, together with transformation and dislocation climb due to absorption of vacancies and atoms from precipitates [13].

4. Simulation of strengthening at $T > 0$ K

At non-zero temperature CRSS due coherent precipitates decreases significantly and this depends on the precipitate size. Furthermore, we found a significantly weaker tendency for bcc-to-fcc phase transformation in Cu at $T > 0$ K. Data for the temperature dependence are presented in Fig. 5 for $D = 2$, 3 and 4 nm. Note the different temperature dependence for small ($D = 2$ nm) and large ($D \geqslant 3$ nm) precipitates. Thus, τ_c, for a small precipitate demonstrates a significant drop at low temperatures, $T < 100$ K, and becomes essentially athermal

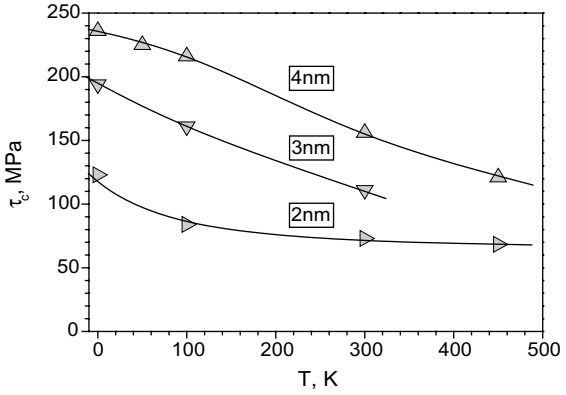

Fig. 5. Critical resolved shear stress as a function of temperature obtained for precipitates of different size.

at $T > 100$ K, whereas, τ_c, for larger precipitates shows a continuous decrease up to at least $T = 450$ K. This can be explained by the difference in the dislocation-precipitate interaction mechanism. Small precipitates are overcome by a simple shear mechanism without phase transformation and dislocation climb. Our simulations show that this mechanism has a weak temperature dependence at temperatures when dislocation motion can be thermally activated, e.g. $T > 100$ K. (For temperature dependence of dislocation Peierls stress in our model, see for example [7].) In contrast, when the mechanism is more complicated and includes competition between different phases and defect absorption or creation, it becomes temperature-dependent, provided these phenomena are characterised by an activation energy which is higher than Peierls energy. As an example of this we considered the case of a 4 nm precipitate at different temperatures. Thus at low temperature ($T < 300$ K) the dislocation absorbed both vacancies (climb up) and atoms (climb down), several vacancies were left in the precipitate at $T = 300$ K and only one was created at $T = 450$ K. A significant transformation towards fcc structure was observed at $T = 0$ (see Section 3 and [13]) but there was no evidence of this at high temperatures. The different mechanisms also affect the dislocation line shape in the glide plane at the critical stress: the Orowan-like shape with $\varphi = 0$ at $\tau_c = 236$ MPa at $T = 0$ K (see Fig. 2) becomes a much smoother line with $\varphi > 0$ at $\tau_c = 121$MPa at $T = 450$ K.

More simulations of different size precipitates and strain rates are necessary to understand the phenomena revealed in this work. However, it is possible even now to predict a different temperature dependence of precipitate-induced strengthening in under-aged or neutron-irradiated Fe–Cu alloys and over-aged or electron-irradiated alloys. The precipitates are small and coherent in the former state and large and/or incoherent in the latter. The former should present a weak temperature dependence above a certain temperature, which characterises the thermally activated mobility of the dislocation and is of the order of 100 K, whereas the latter should give rise to a stronger temperature dependence, which is characteristic of the activation energies of the processes involved, i.e. phase transformation, absorption of atoms and vacancies by the dislocation line, etc.

5. Conclusions

1. The mechanism of dislocation-precipitate interaction depends on the precipitate size D and ambient temperature T.
2. The dislocation overcomes small precipitates ($D \leqslant 2$ nm) at $T = 0$ K by a simple shear mechanism, whereas larger precipitates may transform and the dislocation may climb. The latter effects increase the critical stress τ_c and result in an Orowan-like dislocation shape characterized by zero breaking angle at τ_c, without creation of an Orowan dislocation loop.
3. The dependence of τ_c on D at $T = 0$ K is logarithmic with a possible upper limit around the Orowan stress.
4. At $T > 0$ K the interaction mechanism and τ_c are size and temperature dependent.
5. Small precipitates, which are overcome by a simple shear mechanism, show a strong temperature dependence of τ_c over the range where the dislocation glide is thermally activated ($T \approx 100$ K) and a weak dependence beyond.
6. Larger precipitates, which transform at $T = 0$ K, show a significant and continuous decrease of τ_c and the dislocation climb with increasing T up to 450 K. The phase transformation is suppressed at higher T.
7. The information obtained on the dislocation-precipitate interaction mechanism and its dependence on temperature and precipitate size predicts different temperature behaviour of yield stress between under-aged or neutron-irradiated and over-aged or electron-irradiated Fe–Cu alloys.

Acknowledgements

Research sponsored by the Office of Fusion Energy Sciences and Division of Materials Sciences and Engineering, US Department of Energy under Contract DE-AC05-00OR22725 with UT-Battelle, LLC and supported by a grant from Engineering and Physical Sciences Research Council of the United Kingdom. The authors thank Dr C.A. English and Professor G.R. Odette for stimulating discussions.

References

[1] L.L. Horton, J. Bentley, K. Farrell, J. Nucl. Mater. 108&109 (1982) 222.
[2] G.R. Odette, Scr. Metall. 17 (1982) 1183.
[3] M. Eldrup, B.N. Singh, J. Nucl. Mater. 276 (2000) 269.
[4] J.T. Buswell, P.J.E. Bischler, S.T. Fenton, A.E. Ward, J. Nucl. Mater. 205 (1993) 198.
[5] A.C. Nicol, M.L. Jenkins, M.A. Kirk, Mat. Res. Soc. Proc. 540 (1999) 409.
[6] J.M. Hyde, C.A. English, Mat. Res. Soc. Proc. 650 (2001) R6.6.1.
[7] Yu.N. Osetsky, D.J. Bacon, Model. Simul. Mater. Sci. Eng. 11 (2003) 427.
[8] G.J. Ackland, D.J. Bacon, A.F. Calder, T. Harry, Philos. Mag. A 75 (1997) 713.
[9] A.J. Ackland, G. Tichy, V. Vitek, M.V. Finnis, Philos. Mag. A 56 (1987) 735.
[10] K.C. Russell, L.M. Brown, Acta Metall. 20 (1972) 969.
[11] A.J.E. Foreman, M.J. Makin, Philos. Mag. 14 (1966) 911.
[12] L.M. Brown, B.K. Ham, in: A. Kelly, R.B. Nicholson (Eds.), Strengthening Methods in Crystals, Elsevier, Amsterdam, 1971, p. 12.
[13] Yu.N. Osetsky, D.J. Bacon, J. Nucl. Mater. 323 (2003) 268.
[14] D.J. Bacon, in: B.A. Bilby, K.J. Miller, J.R. Willis (Eds.), Fundamentals of Deformation and Fracture, Cambridge University, Cambridge, 1985, p. 401.
[15] D.J. Bacon, U.F. Kocks, R.O. Scattergood, Philos. Mag. 28 (1973) 1241.